

# Hyperfine interactions in silicon quantum dots

Lucy V. C. Assali,<sup>1</sup> Helena M. Petrilli,<sup>1</sup> Rodrigo B. Capaz,<sup>2</sup> Belita Koiller,<sup>2</sup> Xuedong Hu,<sup>3</sup> and S. Das Sarma<sup>4</sup>

<sup>1</sup>*Instituto de Física, Universidade de São Paulo, CP 66318, 05315-970, São Paulo, SP, Brazil*

<sup>2</sup>*Instituto de Física, Universidade Federal do Rio de Janeiro,  
Caixa Postal 68528, 21941-972 Rio de Janeiro, Brazil*

<sup>3</sup>*Department of Physics, University at Buffalo, SUNY, Buffalo, New York 14260-1500, USA*

<sup>4</sup>*Condensed Matter Theory Center, Department of Physics,  
University of Maryland, College Park, Maryland 20742-4111, USA*

(Dated: February 14, 2019)

We present an all-electron calculation of the hyperfine parameters for conduction electrons in Si, indicating: (i) all parameters scale linearly with the spin density at a <sup>29</sup>Si site; (ii) the isotropic term is over 30 times larger than the anisotropic part; (iii) conduction electron charge density at a Si nucleus is consistent with experimental estimates; (iv) Overhauser fields in natural Si quantum dots (QDs) are two orders of magnitude smaller than in GaAs QDs. This reinforces the outstanding performance of Si in keeping spin coherence and opens access to reliable quantitative information aiming at spintronic applications.

PACS numbers: PACS numbers: 03.67.Lx, 76.30.Pk 71.70.Jp. 71.15.Mb

The great current interest in Si in the context of spintronics and spin quantum computation [1, 2] arise naturally from its perceived technological and fundamental advantages. Technological advantages included scalability and unique material processing capabilities, developed primarily by the well established and, already for half-a-century dominant Si microelectronics industry. The fundamental advantage, which is the key motivation for our work, is the very weak hyperfine coupling in silicon, leading to very long electronic spin coherence times, thus enabling fault-tolerant spin qubit operations. Recent ESR experiments on phosphorus donor electrons in isotopically purified Si show that electron spin coherence times are longer than 60 ms [3]. However, fabricating P donor arrays with the necessary atomic-scale precision [4] is a difficult challenge still to be overcome [5]. An alternative to the Si:P system uses electron spins confined in gate-controlled Si quantum dots (QD) as qubits. There have been extensive experimental studies of few-electron spin dynamics in gated semiconductor (in particular GaAs) QDs for the past ten years [6]. Gated Si QDs have been fabricated and studied as well [7–9]. Recent experiments in these QD systems have shown that single-electron QDs are well within reach in Si [10].

In bulk Si (for Si:P), the most important factor limiting quantum coherence of donor electron spins is their magnetic hyperfine interactions (HFI) with the random <sup>29</sup>Si nuclei in the environment [11–13]. Clearly, accurate knowledge of HFI is required to quantitatively evaluate spin decoherence for an electron confined in a QD and to reliably assess the magnitude of the Overhauser field [14] from the <sup>29</sup>Si nuclear spins in natural Si. However, in spite of the considerable importance of the subject matter, the hyperfine coupling parameters have never before been evaluated for silicon conduction electrons, either bulk or bound to a QD — our work fills this informa-

tion gap.

In this Letter we develop, motivated by spintronic and solid state quantum computing considerations, an ab initio study of the HFI parameters between conduction electrons and <sup>29</sup> Si nuclei. Our results are directly relevant to the prospective application of Silicon as the ideal material of choice in spintronics and spin quantum computation. In addition, they present good agreement with the existing experimental data related to HFI [15–17].

The HFI hamiltonian has the general form

$$H_{\text{HF}} = \mathbf{I} \cdot \mathbf{A} \cdot \mathbf{S}, \quad (1)$$

where  $\mathbf{S}$  and  $\mathbf{I}$  are the electron and nuclear spin operators, and  $\mathbf{A}$  is the HFI tensor. The tensor components for a nucleus at  $\mathbf{R}_I$  can be written in terms of an isotropic term  $a$ , known as Fermi contact term, and of an anisotropic dipolar traceless tensor  $b_{ij}$ :  $A_{ij} = a\delta_{ij} + b_{ij}$ . The labels  $i$  and  $j$  refer to coordinates  $x$ ,  $y$ , and  $z$  taken here along the conventional fcc cubic cell edges. We consider Si with one extra electron at a fixed conduction band minimum  $\mathbf{k}_i$ . The system has axial symmetry with respect to the  $i$ -axis, so that the traceless anisotropic tensor is diagonal and expressed as  $b_{ij} = \text{diag}\{2b, -b, -b\}$ . The hyperfine tensor  $\mathbf{A}$  is thus completely defined by the scalar hyperfine parameters  $a$  and  $b$ , as described in Ref. [18]. Explicit expressions for these parameters [18] are determined by the electron spin density,

$$\rho_S(\mathbf{r}) = \rho_{\uparrow}(\mathbf{r}) - \rho_{\downarrow}(\mathbf{r}). \quad (2)$$

In particular the Fermi contact interaction is proportional to the spin density at the nuclear site,  $\rho_S(\mathbf{R}_I)$ . From  $a$  and  $b$ , given in energy units, one can obtain the equivalent magnetic field created by the nuclear spin acting on an electron spin. Reliable calculation of the HFI parameters require precise values of  $\rho_S(\mathbf{r})$  for all  $\mathbf{r}$ , in particular in the vicinity  $\mathbf{r} \approx \mathbf{R}_I$ .

Our calculations, performed within the Density Functional Theory framework [19], involve the full-potential linearized augmented plane wave method (FP-LAPW) [20], as embodied in the WIEN2k package [21]. This state-of-the-art all-electron methodology includes spin polarization of the core and valence states, spin-orbit coupling, and relativistic effects. No shape assumption (e.g. the usual spherical constrain) to the potential is involved. The generalized gradient approximation is used for the calculation of the exchange-correlation potential [22]. Calculations of HFI of negatively charged bulk silicon are performed for several Si supercell sizes, ranging from  $N = 8$  to 64 atoms, each with a single extra electron. In practice this corresponds to different average electronic densities  $\rho_N = 2e/(N\Omega_{PC})$ , where  $\Omega_{PC}$  is the volume of the Si primitive cell (PC), which contains two atoms. A uniform positive jellium background with density  $|\rho_N|$  is included to cancel the long range multipole interactions of charged supercells [23]. Grids from 8 to 125 k-points are used to sample the irreducible wedge of the Brillouin zone [24], according to the supercell size. The calculation is performed self-consistently until convergence on the total energy and total charge is achieved. This approach realistically describes the electronic properties, and has previously been used to calculate HFI of impurities in semiconductors [25, 26].

We follow a two-step procedure to compute the hyperfine parameters at a given Si site for a supercell with an extra electron: 1) The converged charge density is obtained from a standard spin-polarized self-consistent calculation. 2) This charge density is used to get the potential energy of the Kohn-Sham equation, and the Hamiltonian is written assuming a fixed  $\mathbf{k}_i$  corresponding to one of the six conduction band minima. In this way we constrain the extra electron to a fixed k-point, in analogy with the case of impurities in semiconductors [23, 25, 26]. From the sum over all occupied bands  $n$  of  $|\phi_n^\sigma(\mathbf{r})|^2$  and of  $|\phi_n^{\bar{\sigma}}(\mathbf{r})|^2$  for each spin orientation  $\sigma$  and  $\bar{\sigma}$  (where  $\phi_n^{\sigma,\bar{\sigma}}$  are the Kohn-Sham eigenstates), we obtain the net spin density [Eq.(2)], as described in the appendix of Ref. 25. Note that for neutral bulk Si  $\rho_S = 0$ , so the calculated  $\rho_S(\mathbf{r})$  is entirely due to the added electron. This procedure provides as good quantitative estimates of spin density as possible within available theoretical treatments.

Figure 1 shows the spin density in the (100) crystal plane calculated with an 8-atom supercell for negatively charged Si, where the extra electron is kept at  $\mathbf{k} = \mathbf{k}_z$  at the conduction band edge. Note the anisotropy of the distribution, elongated in the axial  $z$  direction. Comparison of this spin density with the charge density in the same plane for the conduction band  $\mathbf{k}_z$  pseudo-wavefunction, given in Fig. 1(b) of Ref. 27, illustrates the similarity of the two distributions, except for regions just around the atomic sites. This is because results in Ref. 27 were obtained within the pseudopotential approach, where the

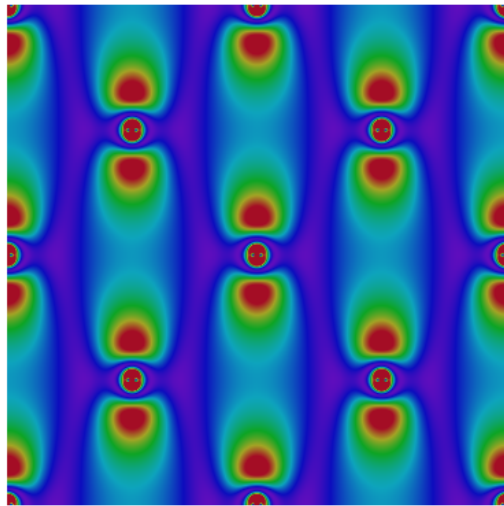


FIG. 1: (Color online) Electron spin density in a (100) plane for bulk Si with an extra electron in the conduction band minimum at  $k_z$ . The vertical axis is  $z$  and the color scheme runs from red (high density) to purple (low density), following the rainbow sequence. The circular high density spots are the Si atomic sites.

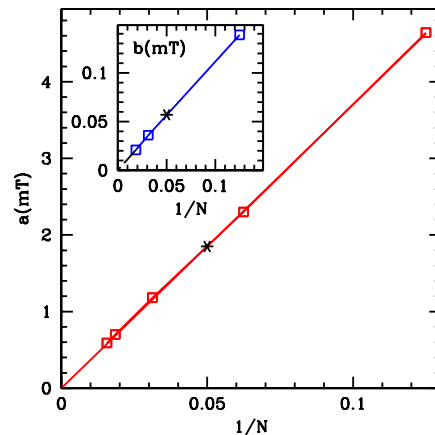


FIG. 2: (Color online) Squares give the calculated hyperfine parameters versus  $1/N$ , where  $N$  is the number of Si atoms in the supercell. The asterisks give the interpolated values expected for natural Si ( $\sim 5\%$  of  $^{29}\text{Si}$ ), with  $a \approx 1.9$  mT and  $b \approx 0.06$  mT. Solid straight lines are  $a_N = (37/N)$  mT and  $b_N = (1.1/N)$  mT, and give a good fits to the data points.

core region potentials are very different from the actual ones. The same similarity is obtained in any other plane. These considerations, and the fact that  $\rho_S(\mathbf{r})$  is nonzero with the added electron, allows us to identify  $\rho_S(\mathbf{r})$  in our all-electron calculation with the charge distribution of the extra electron, which in a one-electron scheme corresponds to  $|\Psi_{k_i}(\mathbf{r})|^2$ , the absolute value of the Bloch function squared.

Figure 2 summarizes the calculated  $^{29}\text{Si}$  HFI in the negatively charged supercells. The hyperfine parameters  $a$  and  $b$  are given as a function of  $1/N$ , showing that they scale linearly with the electronic density. We note that, for natural Si, the isotropic parameter is of the order of a couple of mT, while the anisotropic parameter  $b/a \sim 3\%$  for all  $N$ .

Within a mono-electronic framework, the conduction band wavefunction relative weight at a Si atomic site  $\mathbf{R}_I = 0$  may be quantified by a parameter ( $\eta$ ) defined below [15]. It is widely adopted in experiments and in effective mass calculations. The original definition in a one-electron context and the analogous expression for the all electron framework here are, respectively

$$\eta_{1E} = \frac{|\Psi(0)|^2}{(|\Psi|^2)_{Av}} \Leftrightarrow \eta_{AE} = \frac{\rho_S(0)}{(\rho_S)_{Av}}, \quad (3)$$

where in the denominators  $(Q)_{Av}$  is the average of  $Q$  over the normalization volume. We omit the subscripts “1E” and “AE” below. Ref. [15] inferred  $\eta = 186 \pm 18$  for  $^{29}\text{Si}$  from NMR experiments. Later work [16] identified an error in Ref. 15 and gave a corrected value of  $\eta = 178 \pm 31$ . Ref. [17] deduced  $\eta$  by extrapolating Overhauser shift data and obtained roughly twice the value reported in Ref. [15], with  $\eta \gtrsim 300$ . Our calculation constitutes the first theoretical estimate for  $\eta$  and give  $\eta = 159.4 \pm 4.5$ . The results are presented and compared to the experimental estimates [15, 16] in Fig. 3.

We now consider an electron confined in a gated QD near a [001] interface with a barrier material. In this case the valleys in directions perpendicular to the interface,  $\pm k_z$ , are lower in energy and make up the electronic ground state. By symmetry,  $\rho_S$  is the same for  $k_z$  and  $-k_z$ , so the results here apply to general superposition states involving  $\pm k_z$ . In the envelope function approach, the electron wave function in the QD is given by a bulk state modulated by a slowly varying envelope function  $F(\mathbf{r})$ , with  $\int_{\text{all space}} |F|^2 d\mathbf{r} = 1$ . In the all-electron scheme, the envelope modulation is  $|F|^2$ , since  $|\Psi|^2$  is associated with  $\rho_S$ , while the bulk contribution to the spin density is normalized within a PC, so that the overall spin density in a quantum dot (normalized in all space) is

$$\rho_S^{QD}(\mathbf{r}) = |F(\mathbf{r})|^2 \Omega_{PC} \rho_S^{PC}(\mathbf{r}). \quad (4)$$

In essence our *ab initio* calculation for a supercell of volume  $V$  is equivalent to having a uniform envelope function  $F = 1/\sqrt{V}$  and a bulk spin density normalized in a PC. In a QD,  $F$  is non-uniform and extends over tens of nanometers. However, this change does not affect the calculation for the contact part of the interaction, because both the envelope function and the total spin density are normalized over the QD.

The contact HFI field due to a nuclear spin at  $\mathbf{R}_I$  in a

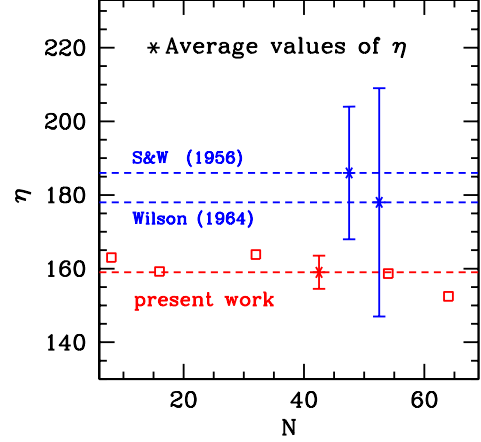


FIG. 3: (Color online) Calculated  $\eta$  for different supercell sizes (red squares). The average value and standard deviation are given by the lowest (red) asterisk and respective error bar. Experimental results are given by the upper (blue) horizontal dashed lines, following the average values of Refs. 15 and 16, labeled S&W (1956) and Wilson (1964), respectively. The error bar for Wilson was obtained as an upper limit of the error estimated from Ref. 16, where  $\eta_{\text{Si}}$  is given in an expression related to  $\eta_{\text{Ge}}$ . The horizontal position of the asterisks is arbitrary, as they represent average values. The estimated value of  $\eta \gtrsim 300$  in Ref. 17 is off the scale here.

QD is

$$a(\mathbf{R}_I) = a_2 |F(\mathbf{R}_I)|^2 \Omega_{PC}, \quad (5)$$

where  $a_2$  is extrapolated from our supercell calculations (see Fig. 2) to a PC (a supercell with  $N = 2$ ). Since we fit our calculations as  $a_N \approx (37/N)$  mT,  $a_2 = 18.5$  mT. The  $a(\mathbf{R}_I)$  thus calculated is the interaction strength of the electron with a particular nucleus at  $\mathbf{R}_I$ . Now if we have a QD where every nucleus has a spin, with the nuclear spins arranged in a fully polarized state, the total HFI  $\mathcal{A}$  is a sum over the whole QD:

$$\mathcal{A} = \sum_{\mathbf{R}_I \in QD} a(\mathbf{R}_I) = 2a_2, \quad (6)$$

where the factor 2 accounts for contributions from the two nuclear sites per PC, and, to an excellent approximation, the envelope is taken to be constant within each elementary PC partitioning the electronic distribution in the QD. The total HFI  $\mathcal{A}$  corresponds to the magnetic field acting on the electron if all nuclear spins in the QD are polarized.

With current interest in constructing single-electron Si QDs in mind, we list in Table I estimates of the relevant Overhauser fields [14] and/or energy scales in Si and GaAs QDs. The random Overhauser field  $\delta\mathcal{A}$  for a high temperature nuclear reservoir is  $\delta\mathcal{A} = \mathcal{A}/\sqrt{N_S}$ ,

host	$\mathcal{N}_T$	$\mathcal{N}_S$	$\mathcal{A}$	$\delta\mathcal{A}$	$T_2^*$
GaAs	$10^6$	$10^6$	92 $\mu\text{eV}$ (3.6 T)	0.092 $\mu\text{eV}$	7.2 ns
Natural Si	$10^5$	5000	210 neV (1.85 mT)	3.0 neV	0.22 $\mu\text{s}$
100% $^{29}\text{Si}$	$10^5$	$10^5$	4.3 $\mu\text{eV}$ (37 mT)	6.1 neV	110 ns
0.01% $^{29}\text{Si}$	$10^5$	50	0.43 neV (3.7 $\mu\text{T}$ )	0.061 neV	11 $\mu\text{s}$

TABLE I: Order of magnitude estimates of HFI that an electron can experience in a Si QD. The columns give the total number  $\mathcal{N}_T$  of nuclei in the dot, the number  $\mathcal{N}_S$  of non-zero spin, the maximum  $\mathcal{A}$  and random  $\delta\mathcal{A} = \mathcal{A}/\sqrt{\mathcal{N}_S}$  Overhauser fields, when the nuclear spins are all aligned or in a random configuration, and the corresponding  $T_2^*$  dephasing time. The estimates for GaAs are given for comparison.

with  $\mathcal{N}_S$  giving the total number of nonzero spin nuclei. The  $T_2^*$  time is the electron spin dephasing time, and is given by  $T_2^* = \hbar/\delta\mathcal{A}$ . The first row of the table shows typical data for a GaAs [28] QD that contains about  $10^6$  nuclei, and is given as a benchmark for comparison. The 2nd row gives the data for a typical natural Si QD with  $10^5$  nuclei (generally Si QDs are more strongly confined than GaAs QDs). With the three orders of magnitude difference in the maximum Overhauser field  $\mathcal{A}$  in GaAs and natural Si, the random fields and  $T_2^*$  are different by about two orders of magnitude. For an isotopically enriched  $^{29}\text{Si}$  sample, the difference goes down to one order of magnitude (3rd row); while for an isotopically enriched  $^{28}\text{Si}$  sample (4th row), the difference goes up to three orders of magnitude. The much smaller possible random Overhauser field in Si QDs leads to much longer inhomogeneous broadening time  $T_2^*$ , ranging from 110 ns for a pure  $^{29}\text{Si}$  dot to 11  $\mu\text{s}$  for a 99.99% purified  $^{28}\text{Si}$  dot. The extended  $T_2^*$  time indicates that in Si coherent electron spin manipulation is possible even without spin echoes that correct the effect of inhomogeneous Overhauser field. Conversely, if an inhomogeneous field is required to manipulate the electron spin states [6, 29], as well as for other spintronic applications [30], in Si such a field probably needs to be applied.

We also estimate the anisotropic HFI of a nuclear spin at  $\mathbf{R}_I$  in the QD by including two contributions. One is the near-field contribution, dominated by the anisotropy of the spin density for  $\mathbf{r} \approx \mathbf{R}_I$ . Taking a small volume  $\Omega \sim \Omega_{PC}$  around  $\mathbf{R}_I$ , containing  $N_\Omega \sim 2$  Si atoms, the near-field contribution is  $\Omega |F(\mathbf{R}_I)|^2 b_{N_\Omega}$ , and the scaling  $b_N = (1.1/N)$  mT can be used. The second is the far-field contribution, which depends on where the nuclear spin is located inside the QD. Our numerical estimates indicate that, for a QD with a radius of 20 nm, the near-field contribution is in the order of  $10^{-4}$  Gauss, about 3% of the contact HFI, as expected. The far-field contribution is even smaller, at only  $\sim 10^{-6}$  Gauss per nuclear spin. In short, in a Si QD where a single electron has a smooth probability distribution, the effect of the anisotropic HFI is negligibly small.

In summary, we have performed a state-of-the-art all-

electron calculation of spin density distributions in Si with an extra electron in a fixed valley at the bottom of the Si conduction band. Our calculated HFI strengths are consistent with existing experimental observations. The theoretical estimate for electron spin  $T_2^*$  time in a natural Si QD is one to two orders of magnitude longer than that in a GaAs QD, and the corresponding electron spin decoherence time should be at least two orders of magnitude longer, formally and quantitatively verifying the advantages of Si as a host material for spin qubits. Moreover, our study also introduces and validates an ab-initio approach to an open theoretical question of key relevance in spin behavior in different host materials, in particular semiconductors, paving the way for such estimates in a variety of systems.

This work was partially supported in Brazil by CNPq, CAPES, FAPESP, and FAPERJ. BK, RBC, and HMP performed this work as part of the INCT Program. XH acknowledges support by NSA/LPS through ARO with grant number W911NF-09-1-0393. SDS acknowledges support by NSA/LPS.

- 
- [1] S. Das Sarma *et al.*, Solid State Commun. **133**, 737 (2004).
  - [2] B.E. Kane, Nature **393**, 133 (1998).
  - [3] A.M. Tyryshkin *et al.*, J. Phys.: Condens. Matter **18**, S783 (2006).
  - [4] B. Koiller, X. Hu, and S. Das Sarma, Phys. Rev. Lett. **88**, 027903 (2002).
  - [5] M. Mitic *et al.*, Nanotechnology **19**, 265201 (2008); A. Fuhrer *et al.*, Nano. Lett. **9**, 707 (2009).
  - [6] R. Hanson *et al.*, Rev. Mod. Phys. **79**, 1217 (2008).
  - [7] M. Friesen *et al.*, Phys. Rev. B **67**, 121301 (2003).
  - [8] H.W. Liu *et al.*, Phys. Rev. B **77**, 073310 (2008).
  - [9] E.P. Nordberg *et al.*, arXiv:0906.3748. To appear in Phys. Rev. B.
  - [10] C.B. Simmons *et al.*, Appl. Phys. Lett. **91**, 213103 (2008).
  - [11] W. M. Witzel, Rogerio de Sousa, S. Das Sarma, Phys. Rev. B **72**, 161306(R) (2005); W.M. Witzel and S. Das Sarma, *ibid.* **74**, 035322 (2006).
  - [12] W.M. Witzel, X. Hu, and S. Das Sarma, Phys. Rev. B **76**, 035212 (2007).
  - [13] J.L. Ivey and R. L. Mieher, Phys. Rev. B **11**, 849 (1975).
  - [14] The Overhauser field is the net field felt by the electron spin due to the distribution of nuclear spins in the sample.
  - [15] R.G. Shulman and B. J. Wyluda, Phys. Rev. **103**, 1127 (1956).
  - [16] D.K. Wilson, Phys. Rev. **134**, A265 (1964). See Refs. [31] and [32] therein.
  - [17] V. Dyakonov and G. Denninger, Phys. Rev. B **46**, 5008(R) (1992).
  - [18] C.G. Van de Walle and P.E. Blöchl, Phys. Rev. B **47**, 4244 (1993).
  - [19] W. Kohn and L. J. Sham, Phys. Rev. **140**, A1133 (1965).
  - [20] D. J. Singh, *Plane waves, Pseudopotentials and the LAPW method* (Kluwer Academic, Norwell, 1994).
  - [21] P. Blaha, K. Schwarz, G.K.H. Madsen, D. Kvasnicka,

- and J. Luitz, WIEN2K, *An Augmented Plane Wave + Local Orbitals Program for Calculating Crystal Properties* (Karlheinz Schwarz, Techn. Universitat Wien, Austria), 2001 (ISBN 3-9501031-1-2).
- [22] J. P. Perdew, K. Burke, and M. Ernzerhof, Phys. Rev. Lett. **77**, 3865 (1996).
  - [23] L. V. C. Assali *et al.*, Phys. Rev. B **69**, 155212 (2004).
  - [24] H. J. Monkhorst and J. D. Pack, Phys. Rev. B **13**, 5188 (1976).
  - [25] R. Larico *et al.*, Phys. Rev B **79**, 115202 (2009).
  - [26] R. Larico *et al.*, Appl. Phys. Lett. **84**, 720 (2004); F. Ayres *et al.*, *ibid* **88**, 011918 (2006).
  - [27] B. Koiller *et al.*, Phys. Rev. B **70**, 115207 (2004).
  - [28] D. Paget *et al.*, Phys. Rev. B **15**, 5780 (1977).
  - [29] J.R. Petta *et al.*, Science **309**, 2180 (2005).
  - [30] I. Zutic, J. Fabian, and S. Das Sarma, Rev. Mod. Phys. **76**, 323 (2004).